

# Inside versus Outside: Ion Redistribution in Nitric Acid Reacted Sea Spray Aerosol Particles as Determined by Single Particle Analysis

Andrew P. Ault,<sup>†,¶</sup> Timothy L. Guasco,<sup>‡,⊥</sup> Olivia S. Ryder,<sup>‡</sup> Jonas Baltrusaitis,<sup>†,#</sup> Luis A. Cuadra-Rodriguez,<sup>‡</sup> Douglas B. Collins,<sup>‡</sup> Matthew J. Ruppel,<sup>‡</sup> Timothy H. Bertram,<sup>‡</sup> Kimberly A. Prather,<sup>\*,‡,§</sup> and Vicki H. Grassian<sup>\*,†</sup>

<sup>†</sup>Department of Chemistry, University of Iowa, Iowa City, Iowa 52242, United States

<sup>‡</sup>Department of Chemistry and Biochemistry, University of California, San Diego, La Jolla, California 92093, United States

<sup>§</sup>Scripps Institution of Oceanography, University of California, San Diego, La Jolla, California 92093, United States

## Supporting Information

**ABSTRACT:** Single particle analysis of individual sea spray aerosol particles shows that cations (Na<sup>+</sup>, K<sup>+</sup>, Mg<sup>2+</sup>, and Ca<sup>2+</sup>) within individual particles undergo a spatial redistribution after heterogeneous reaction with nitric acid, along with the development of a more concentrated layer of organic matter at the surface of the particle. These data suggest that specific ion and aerosol pH effects play an important role in aerosol particle structure in ways that have not been previously recognized.

The heterogeneous chemistry of sea spray particles with nitrogen oxides has been studied in both the laboratory and field.<sup>1–3</sup> The growth of particulate nitrate concomitant with the loss of chloride, along with the formation of important chlorine-containing gas-phase molecules, following heterogeneous reaction of nitrogen oxides with sea spray aerosol (SSA) is well-known.<sup>2,4,5</sup> The displacement of chloride by nitrate in the heterogeneous reaction of nitric acid with sodium chloride, Reaction 1, in sea spray aerosol (SSA) particles is important in atmospheric chemistry due to the loss of nitrogen oxides from the gas phase into the aerosol phase, and subsequent changes to SSA properties.<sup>2,5</sup>



However, as discussed here, little is known about how this anion displacement reaction affects the distribution of cations and other chemical constituents within a phase state of individual SSA particles. Using single particle analysis of unreacted and nitric acid reacted SSA particles, it is shown here for the first time that there is a large change in the internal structure and redistribution of cations in individual SSA particles as they undergo reaction, an unexpected and surprising result. Additionally, particles no longer undergo dehydration and crystallization processes (efflorescence) following heterogeneous reaction, as suggested by the spherical, not cubic, morphology seen in TEM (*vide infra*).<sup>6,7</sup>

Since most laboratory studies of Reaction 1 and other heterogeneous reactions are done on simple models for SSA particles, typically consisting of pure sodium chloride or sodium chloride mixed with sodium dodecyl sulfate, a surfactant molecule,<sup>1,8,9</sup> little is known about the reactivity of more realistic

SSA particles. However, SSA particles are more complex mixtures containing other species that include additional inorganic cations (Mg<sup>2+</sup>, Ca<sup>2+</sup>, and K<sup>+</sup>) and anions (SO<sub>4</sub><sup>2-</sup>), as well as multicomponent organic species which are transferred to the SSA from the sea surface microlayer.<sup>10–12</sup> Furthermore, most laboratory studies are often done using bulk, multiparticle methods of analysis. Therefore, there is a disconnect between transferring the knowledge gained from fundamental laboratory studies using simple model systems and bulk analysis to study these reactions to atmospheric aerosols measured in field studies using single particle methods.<sup>2,10</sup>

To bridge this gap, SSA particles generated under real-world conditions using natural seawater and a unique ocean-atmosphere facility equipped with actual breaking waves or a marine aerosol reference tank (MART) that replicates those conditions were exposed to nitric acid *in situ* in a flow tube.<sup>10,13</sup> Details of this ocean-in-a-lab approach have been previously described in Prather et al.<sup>10</sup> Important aspects related to the current heterogeneous reaction study are given in the Supporting Information (SI). Several different particle types were identified, with the majority of particles studied herein existing as mixtures of inorganic ions (Na<sup>+</sup>, Mg<sup>2+</sup>, K<sup>+</sup>, Ca<sup>2+</sup>, Cl<sup>-</sup>, and SO<sub>4</sub><sup>2-</sup>) and organic material.<sup>10,14</sup> This type of particle is referred to as sea salt mixed with organic carbon (SS-OC) and represents >50% of particles in the size range critical to heterogeneous reactions in the marine atmosphere (particle diameters between 0.3 to 2.0 μm) under a range of seawater conditions.<sup>10,15</sup> Particles analyzed in this study were 0.3–2.0 μm for both reacted and unreacted particles. Particles generated using the ocean-atmosphere facility were reacted *in situ* for 2–8 min at concentrations of HNO<sub>3</sub> higher than the atmosphere (71–127 ppbv), to simulate long-term atmospheric processing, and then analyzed by microscopy. Those using the MART tank were reacted for 2 min at 57 ppbv HNO<sub>3(g)</sub> before ATOFMS analysis. Particles were collected for off-line analysis at 60% RH and sampled by the ATOFMS at 90–100% RH.

Individual SS-OC particles with and without reaction can then be analyzed both in real-time by aerosol time-of-flight mass spectrometry (ATOFMS) and after impaction on transmission electron microscopy (TEM) grids for high angle annular dark

Received: July 16, 2013

Published: September 12, 2013

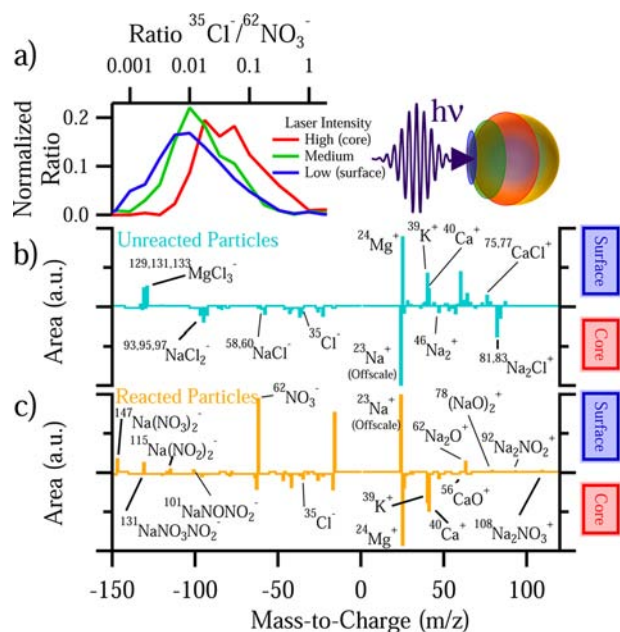


**Figure 1.** (a) Ratio of  $^{35}\text{Cl}^-$  to  $^{62}\text{NO}_3^-$  in reacted particles for different laser intensities and schematic showing degree of particle desorption/ionization as a function of laser intensity. Subtraction spectra showing surface versus core enhanced ions for (b) unreacted and (c) reacted particles.

field scanning transmission electron microscopy analysis coupled with energy dispersive X-ray (EDX) analysis and electron energy loss spectroscopy (EELS).<sup>10,14</sup> These individual particle methods can be used to gain additional insights into these reactions. ATOFMS can use total spectrum ion intensities as a proxy for the power of the desorption/ionization laser, and the ratio of surface to bulk ions generated can be probed (diagram in Figure 1).<sup>16</sup> Subtraction of these mass spectra shows the segregation of specific ions between the particle core and surface change upon reaction. For example, Figure 1a shows that chloride and nitrate are not evenly distributed throughout the particle following reaction with nitric acid. Instead, nitrate is enhanced in the interfacial region away from the particle core as a result of heterogeneous chemistry,<sup>17,18</sup> with chloride present within the core. Additionally, the predominant cations in seawater are either enhanced at the surface ( $\text{Ca}^{2+}$ ,  $\text{Mg}^{2+}$ , and  $\text{K}^+$ ) or depleted ( $\text{Na}^+$ ), as shown for unreacted particles in Figure 1b.<sup>19</sup> What is most unexpected is the fact that there is a redistribution of the cations between the core and surface after heterogeneous reaction with nitric acid (Figure 1c). In particular, before reaction,  $\text{Ca}^{2+}$ ,  $\text{Mg}^{2+}$ , and  $\text{K}^+$  are enhanced at the surface, while  $\text{Na}^+$  is mostly present in the core.<sup>20</sup> Whereas after reaction,  $\text{Na}^+$  and sodium clusters along with nitrate are enhanced at the surface and  $\text{Mg}^{2+}$ ,  $\text{K}^+$ , and  $\text{Ca}^{2+}$

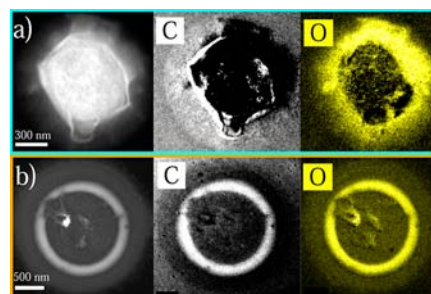


**Figure 3.** Energy Filtered (EF) TEM images of (a) an unreacted sea salt particle (secondary electron, C, and O) and (b) a reacted sea salt particle after vaporization (secondary electron, C, and O).

are present mainly within the core. The redistribution of cations was further probed by elemental mapping using TEM-EDX analysis, as shown in Figure 2. Ion redistribution within individual particles is easily seen when comparing unreacted (Figure 2a) to reacted particles (Figure 2b). Unreacted particles have crystallized and undergone dehydration in the vacuum environment of the TEM. There is a  $\text{NaCl}$  core and  $\text{Mg}$ ,  $\text{K}$ ,  $\text{Ca}$ ,  $\text{S}$ , at the surface following crystallization.<sup>14,21</sup> Organic matter is also enhanced at the surface of the particles, as shown previously.<sup>22</sup> However, the reacted particles clearly show a very different behavior in that  $\text{Ca}$ ,  $\text{Mg}$ ,  $\text{K}$ ,  $\text{Cl}$ , and  $\text{S}$ , in the form of sulfate as determined by EDX,<sup>14</sup> are depleted at the surface of the particle,<sup>17,23</sup> while  $\text{Na}$  is enhanced at the surface of the still spherical particle. Additional evidence is seen in XPS analysis of substrate deposited particles (Figure S1 in SI). Taken together, these data (TEM-EDX and XPS) provide confirmation that the heterogeneous reaction with nitric acid leads to ion redistribution and change in internal structure.

It is difficult to obtain clear images of elemental C with EDX with the carbon-containing TEM grid. Thus, TEM-EELS images were obtained for both reacted and unreacted particles focusing on three elements: C, O, and Cl (Figure 3). For the unreacted particles (Figure 3a), Cl is again seen within the core with a diffuse layer of C and O (organic carbon) indicative of a dehydrated particle. The reacted particle however shows a very different internal orientation with a much narrower, less diffuse organic (C and O) ring ca. 50–100 nm thick on the edge of the particle (Figure 3b). Based on scanning transmission X-ray microscopy with near edge X-ray absorption fine structure spectroscopy, carboxylate ( $\text{COO}^-$ ) groups are one of the major functional groups present in the organic matter.<sup>10,14</sup> It should be noted that the reacted particle is very sensitive to beam damage because the particle has not crystallized and can be volatilized by the electron beam. (Details of the beam damage to particles are included in the SI.) Based on the ATOFMS spectra, TEM-EDX, and TEM-EELS data, the chloride ion is still present within the

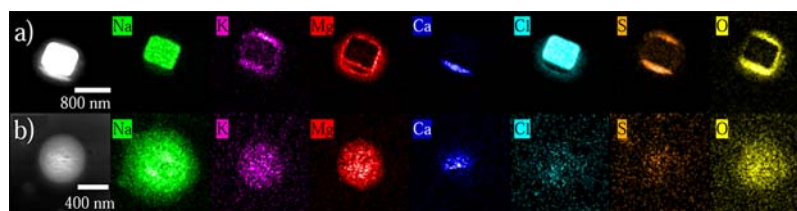


**Figure 2.** High angle annular dark field scanning transmission electron microscopy (HAADF-STEM) images and energy dispersive X-ray (EDX) elemental maps of  $\text{Na}$ ,  $\text{K}$ ,  $\text{Mg}$ ,  $\text{Ca}$ ,  $\text{Cl}$ ,  $\text{S}$ , and  $\text{O}$  for (a) an unreacted sea spray aerosol containing sea salts and organic species (denoted as an SS-OC type particle) and (b) a reacted SS-OC particle.

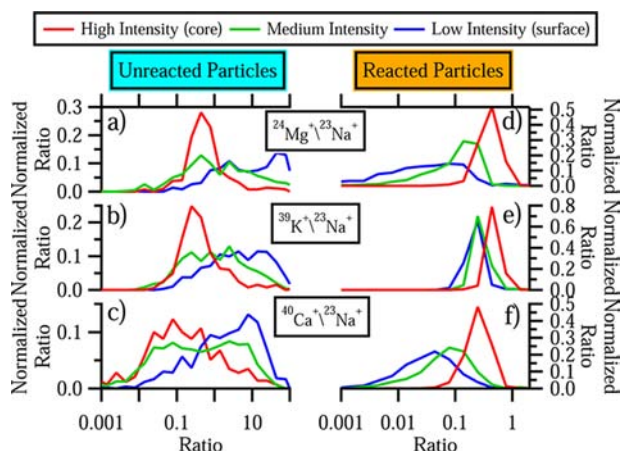


**Figure 4.** Ratios of peak areas for different cations to  $^{23}\text{Na}^+$  as a function of laser intensity for unreacted particles (a)  $^{24}\text{Mg}^+$ , (b)  $^{39}\text{K}^+$ , (c)  $^{40}\text{Ca}^+$  and reacted particles (d)  $^{24}\text{Mg}^+$ , (e)  $^{39}\text{K}^+$ , (f)  $^{40}\text{Ca}^+$ .

core of the particle despite the ion rearrangement and formation of a well-defined enhanced organic carbon layer after reaction with nitric acid.

To verify that the relative distribution of inorganic cations,  $\text{Na}^+$ ,  $\text{Mg}^{2+}$ ,  $\text{K}^+$ , and  $\text{Ca}^{2+}$  is not a function of the offline analysis leading to artifacts after collection and dehydration, comparisons of ion ratios were made at different laser intensities using the ATOFMS in Figure 4 (using the same method as that described for Figure 1a). Since these online results are not subject to the potential challenges of offline storage and analysis, though some water loss can occur in the aerodynamic lens inlet,<sup>24</sup> their use in confirming what is observed with microscopy techniques is essential. As shown here, the ratio of other cations to  $^{23}\text{Na}^+$  is shown for  $^{24}\text{Mg}^+$  (Figure 4a),  $^{39}\text{K}^+$  (Figure 4b), and  $^{40}\text{Ca}^+$  (Figure 4c). For all of the unreacted particles, the lowest ratios (i.e., highest relative amount of Na) were observed in the core of the particle and the relative amount of each cation increased approaching the surface, indicating that  $\text{Mg}^{2+}$ ,  $\text{K}^+$ , and  $\text{Ca}^{2+}$  were enhanced at the surface of the particles. For the reacted particles (Figure 4d–f) the opposite trend is observed and the highest ratios (i.e., least Na) were observed at the particle cores. The shift in ratio is greatest for  $\text{Ca}^{2+}$  (suggesting it is spatially located within the core of the reacted particle), which suggests the precipitation of  $\text{CaSO}_4$  in the core of the aqueous portion of the reacted particle.  $\text{Mg}^{2+}$  and  $\text{K}^+$  have similar shifts to the core, but not as much of a redistribution as  $\text{Ca}^{2+}$  because they do not precipitate out and likely exist as aqueous, dissociated  $\text{Mg}^{2+}$  and  $\text{K}^+$ . Furthermore, the observed ion distributions are much sharper for the reacted particles, which would be expected for a more ordered, heterogeneous internal structure (versus broad distributions for a homogeneous mixture within an aqueous solution as seen in Figure 4a–c).

Two important questions need to be addressed regarding the changes observed after reaction with nitric acid: First, why do  $\text{Ca}^{2+}$  and  $\text{Mg}^{2+}$  relocate to the core of the particle? Second, why does the compact organic ring form? Regarding the organic ring forming a more dense surface layer, after reaction of SSA in the atmosphere with acids, the pH in SSA particles drops dramatically from ca. 8 (matching the slight alkalinity of seawater) to ca. 3 (highly acidic).<sup>25</sup> Likewise the acidification of the nascent SSA particles in the flow tube likely causes the pH to drop below the isoelectric point of the organic material leading to isoelectric precipitation and the formation of a new phase.

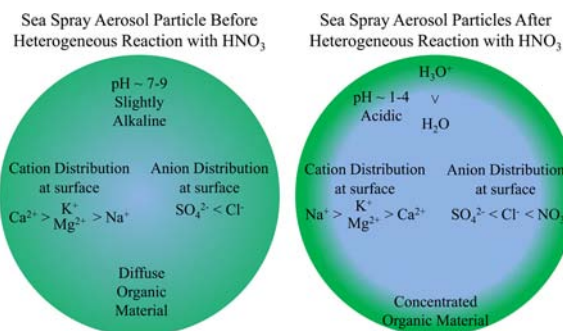


**Figure 5.** Schematic showing ion distributions of SSA particles before and after reaction with nitric acid.

Further discussion of the pH and a comparison to atmospheric conditions are included in the SI. Interestingly, it has been recently observed that the nitrate ion can bind to carboxylic acid groups and become enhanced in an organic phase.<sup>26</sup> This was shown previously during a liquid–liquid separation through a series of studies using mixtures of  $\text{NaNO}_3$ , water, and glycerol,<sup>26</sup> but this has not been shown for relevant and more complex SSA particles. Additionally, similar studies with  $\text{NaCl}$ /water/glycerol mixtures showed no phase separation or chloride enhancement near the surface.<sup>27</sup> The transition to a pH below the  $\text{pK}_a$  of the carboxylate group leads to two important changes. First, the divalent cations,  $\text{Mg}^{2+}$  and  $\text{Ca}^{2+}$ , are more likely to be solvated in the aqueous phase, as they no longer can chelate to the carboxylate anion. The greater enthalpies of hydration for  $\text{Mg}^{2+}$  and  $\text{Ca}^{2+}$  versus  $\text{Na}^+$  explain why they may be relatively enhanced in the aqueous core.<sup>28,29</sup>  $\text{Na}^+$  may also bind preferentially with the phase separated organic species at the surface. Second, the nitrate anion can now hydrogen bond with the carboxylic acid groups leading to some enrichment in the organic phase. Hydrogen bonding with nitrate should be stronger than chloride due to the higher charge density of the oxygen atoms in the nitrate anion. Prior to reaction  $\text{Ca}^{2+}$  and  $\text{SO}_4^{2-}$  are both in solution, in part due to the fact that  $\text{MgCl}_2$  enhances the solvation of  $\text{CaSO}_4$  in  $\text{NaCl}$  solutions at seawater molality.<sup>30</sup> After reaction and loss of  $\text{Cl}^-$ , this effect is no longer operable leading to precipitation of  $\text{CaSO}_4(\text{s})$ . The remaining  $\text{Cl}^-$ ,  $\text{Mg}^{2+}$ , and  $\text{K}^+$  are enhanced in the interior of the particle. Phase separated systems have also shown increased formation of ion pairs between  $\text{Na}^+$  and  $\text{NO}_3^-$  in the organic phase.<sup>26</sup>

Therefore, the current results of particles collected or sampled at ambient RH and concentrations similar to exposure of hours over the SSA particle atmospheric lifetime of days are the first direct observations of SSA particles undergoing such a cation rearrangement and phase separation. This provides direct evidence to support predictions that liquid–liquid phase separations occur under atmospheric conditions.<sup>31,32</sup>

Figure 5 shows a schematic cartoon of the distribution of cations, anions, and organic matter within an SSA particle before and after reaction with nitric acid. The observations of ion redistribution in, and organic concentration at the surface of, SSA particles after reaction with nitric acid have important implications for atmospheric chemistry. The ordering of organic coatings can impact trace gas uptake, and subsequently impact trace gas budgets of  $\text{O}_3$  and  $\text{NO}_x$ .<sup>33</sup> Even the climate models with the most detailed representations of aerosol chemical composition often treat ambient SSA particles as a simple aqueous  $\text{NaCl}$  solution;<sup>34</sup> these results demonstrate that this simplification may introduce error regarding how the particles

undergo reactions and take up water. Just as in biological systems, complexity matters. These measurements make clear the need to apply fundamental chemical understanding to the complexity of the ambient atmosphere and atmospheric aerosols. Furthermore, specific ion effects are well-known in biology and have been shown for simple aqueous salt solutions.<sup>17,23</sup> These studies of simple systems can be enormously important in providing fundamental information on atmospheric systems,<sup>28,35–37</sup> but questions remain about how well they can reproduce the complexity of SSA particles. There is little understanding of these effects in more complex realistic atmospheric aerosols. Additional insights into these effects will provide important and much needed information on atmospheric aerosols and their impact on the environment and climate.

## ■ ASSOCIATED CONTENT

### ■ Supporting Information

Further information on the experiment, EDX spectra and maps, and XPS data showing relative ion concentrations at the particle surface are given in the Supporting Information. This material is available free of charge via the Internet at <http://pubs.acs.org>.

## ■ AUTHOR INFORMATION

### Corresponding Authors

vicki-grassian@uiowa.edu  
kprather@ucsd.edu

### Present Addresses

<sup>¶</sup>Department of Environmental Health Science and Department of Chemistry, University of Michigan, Ann Arbor, MI, 48109.

<sup>†</sup>Department of Chemistry, Millikin University, Decatur, IL, 62522.

<sup>#</sup>Faculty of Science and Technology, University of Twente, Enschede, Netherlands.

### Notes

The authors declare no competing financial interest.

## ■ ACKNOWLEDGMENTS

The authors thank all collaborators involved with the CAICE intensive campaign and the SIO Hydraulics Laboratory staff. The authors acknowledge the Central Microscopy Research Facility at the University of Iowa for assistance. This work was funded by the National Science Foundation through the Center for Chemical Innovation program, CHE1305427.

## ■ REFERENCES

- (1) Finlayson-Pitts, B. J. *Phys. Chem. Chem. Phys.* **2009**, *11*, 7760.
- (2) Abbatt, J. P. D.; Lee, A. K. Y.; Thornton, J. A. *Chem. Soc. Rev.* **2012**, *41*, 6555.
- (3) Bertram, T. H.; Thornton, J. A. *Atmos. Chem. Phys.* **2009**, *9*, 8351.
- (4) Vogt, R.; Elliott, C.; Allen, H. C.; Laux, J. M.; Hemminger, J. C.; Finlayson-Pitts, B. J. *Atmos. Environ.* **1996**, *30*, 1729.
- (5) Gard, E. E.; Kleeman, M. J.; Gross, D. S.; Hughes, L. S.; Allen, J. O.; Morrical, B. D.; Ferguson, D. P.; Dienes, T.; Galli, M. E.; Johnson, R. J.; Cass, G. R.; Prather, K. A. *Science* **1998**, *279*, 1184.
- (6) Lu, P. D.; Wang, F.; Zhao, L. J.; Li, W. X.; Li, X. H.; Dong, J. L.; Zhang, Y. H.; Lu, G. Q. *J. Chem. Phys.* **2008**, *129*, 104509.
- (7) Kim, H.; Lee, M. J.; Jung, H. J.; Eom, H. J.; Maskey, S.; Ahn, K. H.; Ro, C. U. *Atmos. Environ.* **2012**, *60*, 68.
- (8) Krueger, B. J.; Grassian, V. H.; Iedema, M. J.; Cowin, J. P.; Laskin, A. *Anal. Chem.* **2003**, *75*, 5170.
- (9) ten Brink, H. M. *J. Aerosol Sci.* **1998**, *29*, 57.
- (10) Prather, K. A.; Bertram, T. H.; Grassian, V. H.; Deane, G. B.; Stokes, M. D.; DeMott, P. J.; Aluwihare, L. I.; Palenik, B. P.; Azam, F.; Seinfeld, J. H.; Moffet, R. C.; Molina, M. J.; Cappa, C. D.; Geiger, F. M.;

Roberts, G. C.; Russell, L. M.; Ault, A. P.; Baltrusaitis, J.; Collins, D. B.; Corrigan, C. E.; Cuadra-Rodriguez, L. A.; Ebben, C. J.; Forestieri, S. D.; Guasco, T. L.; Hersey, S. P.; Kim, M. J.; Lambert, W. F.; Modini, R. L.; Mui, W.; Pedler, B. E.; Ruppel, M. J.; Ryder, O. S.; Schoepp, N. G.; Sullivan, R. C.; Zhao, D. *Proc. Natl. Acad. Sci. U.S.A.* **2013**, *110*, 7550.

(11) Pilson, M. E. Q. *An introduction to the chemistry of the sea*; Prentice Hall: 1998.

(12) Ault, A. P.; Zhao, D.; Ebben, C. J.; Tauber, M. J.; Geiger, F. M.; Prather, K. A.; Grassian, V. H. *Phys. Chem. Chem. Phys.* **2013**, *15*, 6206.

(13) Stokes, M. D.; Deane, G. B.; Prather, K. A.; Bertram, T. H.; Ruppel, M. J.; Ryder, O. S.; Brady, J. M.; Zhao, D. *Atmos. Meas. Tech.* **2013**, *6*, 1085.

(14) Ault, A. P.; Moffet, R.; Baltrusaitis, J.; Collins, D. B.; Ruppel, M. J.; Cuadra-Rodriguez, L. A.; Zhao, D.; Guasco, T. L.; Ebben, C. J.; Geiger, F. M.; Bertram, T. H.; Prather, K. A.; Grassian, V. H. *Environ. Sci. Technol.* **2013**, *47*, 5603.

(15) O'Dowd, C. D.; De Leeuw, G. *Philos. Trans. R. Soc. London, Ser. A* **2007**, *365*, 1753.

(16) Zelenyuk, A.; Yang, J.; Song, C.; Zaveri, R. A.; Imre, D. *J. Phys. Chem. A* **2008**, *112*, 669.

(17) Jubb, A. M.; Hua, W.; Allen, H. C. In *Annual Review of Physical Chemistry*; Johnson, M. A., Martinez, T. J., Eds.; Annual Reviews: Palo Alto, CA, 2012; Vol. 63, p 107.

(18) Miller, Y.; Thomas, J. L.; Kemp, D. D.; Finlayson-Pitts, B. J.; Gordon, M. S.; Tobias, D. J.; Gerber, R. B. *J. Phys. Chem. A* **2009**, *113*, 12805.

(19) Casillas-Ituarte, N. N.; Callahan, K. M.; Tang, C. Y.; Chen, X. K.; Roeselova, M.; Tobias, D. J.; Allen, H. C. *Proc. Natl. Acad. Sci. U.S.A.* **2010**, *107*, 6616.

(20) Hua, W.; Jubb, A. M.; Allen, H. C. *J. Phys. Chem. Lett.* **2011**, *2*, 2515.

(21) Li, J.; Anderson, J. R.; Buseck, P. R. *J. Geophys. Res.-Atmos.* **2003**, *108*, D002106.

(22) Tervahattu, H.; Hartonen, K.; Kerminen, V. M.; Kupiainen, K.; Aarnio, P.; Koskentalo, T.; Tuck, A. F.; Vaida, V. *J. Geophys. Res.-Atmos.* **2002**, *107*, 4053.

(23) Jubb, A. M.; Hua, W.; Allen, H. C. *Acc. Chem. Res.* **2012**, *45*, 110.

(24) Zelenyuk, A.; Imre, D.; Cuadra-Rodriguez, L. A. *Anal. Chem.* **2006**, *78*, 6942.

(25) Keene, W. C.; Pszenny, A. A. P.; Maben, J. R.; Stevenson, E.; Wall, A. *J. Geophys. Res.-Atmos.* **2004**, *109*, 307.

(26) Yu, J. Y.; Zhang, Y.; Zeng, G.; Zheng, C. M.; Liu, Y.; Zhang, Y. H. *J. Phys. Chem. B* **2012**, *116*, 1642.

(27) Choi, M. Y.; Chan, C. K. *Environ. Sci. Technol.* **2002**, *36*, 2422.

(28) Uejio, J. S.; Schwartz, C. P.; Duffin, A. M.; Drisdell, W. S.; Cohen, R. C.; Saykally, R. J. *Proc. Natl. Acad. Sci. U.S.A.* **2008**, *105*, 6809.

(29) Schmid, R.; Miah, A. M.; Sapunov, V. N. *Phys. Chem. Chem. Phys.* **2000**, *2*, 97.

(30) Kumar, A.; Shukla, J.; Dangar, Y.; Mohandas, V. P. *J. Chem. Eng. Data* **2010**, *55*, 1675.

(31) You, Y.; Renbaum-Wolff, L.; Carreras-Sospedra, M.; Hanna, S. J.; Hiranuma, N.; Kamal, S.; Smith, M. L.; Zhang, X.; Weber, R. J.; Shilling, J. E.; Dabdub, D.; Martin, S. T.; Bertram, A. K. *Proc. Natl. Acad. Sci. U.S.A.* **2012**, *109*, 13188.

(32) Reid, J. P.; Dennis-Smith, B. J.; Kwamena, N. O. A.; Miles, R. E. H.; Hanford, K. L.; Homer, C. J. *Phys. Chem. Chem. Phys.* **2011**, *13*, 15559.

(33) McNeill, V. F.; Patterson, J.; Wolfe, G. M.; Thornton, J. A. *Atmos. Chem. Phys.* **2006**, *6*, 1635.

(34) Bauer, S. E.; Wright, D. L.; Koch, D.; Lewis, E. R.; McGraw, R.; Chang, L. S.; Schwartz, S. E.; Ruedy, R. *J. Geophys. Res.-Atmos.* **2008**, *8*, 6003.

(35) Jungwirth, P. *Faraday Discuss.* **2009**, *141*, 9.

(36) Tian, C. S.; Byrnes, S. J.; Han, H. L.; Shen, Y. R. *J. Phys. Chem. Lett.* **2011**, *2*, 1946.

(37) Mishra, H.; Nielsen, R. J.; Enami, S.; Hoffmann, M. R.; Colussi, A. J.; Goddard, W. A., III. *Int. J. Quantum Chem.* **2013**, *113*, 413.